energies

MDPI

Supplementary Materials

Strategies towards Cost Reduction in the Manufacture of Printable Perovskite Solar Modules

Dena Pourjafari [1,*], Simone M. P. Meroni [2,*], Diecenia Peralta Domínguez [1], Renán Escalante [1], Jenny Baker [2], Alessary Saadi Monroy [1], Adrian Walters [2], Trystan Watson [2] and Gerko Oskam [1,*]

[1] Departamento de Física Aplicada, CINVESTAV-IPN, Mérida 97310, Yucatán, Mexico; diecenia.peralta@cinvestav.mx (D.P.D.); renan.escalante@cinvestav.mx (R.E.); alessary.sm@gmail.com (A.S.M.)

[2] SPECIFIC IKC, Materials Research Centre, College of Engineering Swansea University Bay Campus Fabian Way, Swansea SA1 8EN, UK; j.baker@swansea.ac.uk (J.B.); a.s.walters@swansea.ac.uk (A.W.); t.m.watson@swansea.ac.uk (T.W.)

* Correspondence: dpourjafari@cinvestav.mx (D.P.); s.m.p.meroni@swansea.ac.uk (S.M.P.M.); gerko.oskam@cinvestav.mx (G.O.); Tel.: +52-999-942-9400 (ext. 2280) (D.P.); +44(0)-179-229-5509 (S.M.P.M.)

Printing is a replication process in which printable ink is applied to a substrate in order to transmit information in a repeatable manner using an image-carrying medium. Over the years, a number of printing technologies have been developed to pattern a wide range of electronic materials on diverse substrates. In general, printable electronics are obtained via replicating a pattern using functional materials inks or pastes. There are several printing methods available for the fabrication of printable electronics, such as gravure printing, flexography printing, inkjet printing, screen printing, among all. Each technique has its benefits and drawbacks. In this work, we have focused on screen printing techniques due to the advantages such as easy operation, low capital cost and low maintenance cost, low volume of wastes, and scalability.

Citation: Pourjafari, D.; Meroni, S.M.P.; Peralta Domínguez, D.; Escalante, R.; Baker, J.; Saadi Monroy, A.; Walters, A.; Watson, T.; Oskam, G. Strategies Towards Cost Reduction in the Manufacture of Printable Perovskite Solar Modules. *Energies* **2022**, *15*, 641. https://doi.org/10.3390/en15020641

Academic Editor: Jürgen Heinz Werner

Received: 10 December 2021
Accepted: 11 January 2022
Published: 17 January 2022

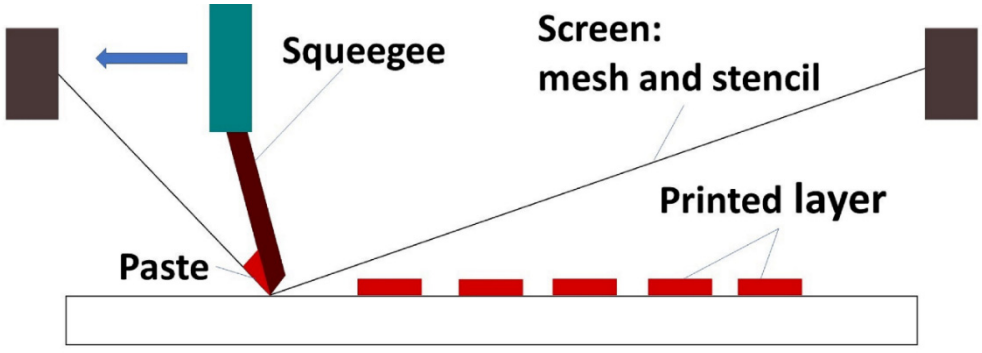

Figure S1. Schematic of the screen-printing method.

The screen-printing technique utilizes a masked screen, commonly made from a metal wire, polymer, or silk mesh, to transfer an image or pattern of the ink onto a substrate. A wide variety of functional pastes and substrates (rigid or flexible) can be used for this technique. During printing, the paste is pushed with a squeegee through a fine screen. The non-image areas of the screen are covered with emulsion. The print quality and homogeneity are determined by the fineness of the screen, the thickness of the emulsion, the degree of the open area of the screen, the correct viscosity and particle size distribution of the paste, the speed, and angle of the squeegee, and the distance between the screen and the substrate.

Table S1. Design parameters for R and S modules.

Module design parameters	R-Module	S-Module
Device Size (cm^2)	27.5 × 21	16.5 × 22
Device area (cm^2)	577.5	363
Total active area (cm^2)	198	224.2
Dead area (cm^2)	379.5	138.8
Active area width (mm)	5	5.2
Right and left margins (mm)	19	10.5
Top and bottom margins (mm)	15	11.5
Single cell length (mm)	180	196
Cell number	22	22
Distance between adjacent cells (mm)	6	1.3
Printed area for BL (cm^2)	577.5	363
Printed area for TiO_2 (cm^2)	198	282
Printed area for ZrO_2 (cm^2)	327	310
Printed area for Carbon (cm^2)	402.6	314
Thickness of BL (nm)	50	50
Thickness of TiO_2 (μm)	0.8	0.8
Thickness of ZrO_2 (μm)	1.2	1.2
Thickness of Carbon (μm)	12	12
Amount of solution for BL (mL)	25	20
Amount of perovskite solution (mL)	0.9	0.9
Efficiency (%)	6.8	7.9
Output power (w)	1.34	1.77

Tables S2 and S4 represent the calculations for the cost of raw materials used in the Registration and Scribing modules, respectively. In these tables, the first column shows the compartments used in device architecture. The second column represents the raw materials that are used to obtain a corresponding compartment. The third column shows the material cost in US dollars per kilogram. These prices have obtained using Sigma Aldrich and local suppliers' websites. The fourth column shows the quantity of each raw material (kg) that is required for the module manufacture (Registration module in Table S2, and Scribing module in Table S4). These quantities are based on experimental procedures and depend on the module's design and dimension (see Figure 2 and Table S1). The last column shows the cost of each raw material required for the module's fabrication in US dollars. Therefore, the total cost of required raw materials to manufacture the modules is obtained from the sum of the values of the last column.

Tables S3 and S5 represent the calculations for the cost of processes used in the Registration and Scribing modules, respectively. In these tables, the first column shows the manufacturing step. The second column represents the experimental procedures for each manufacturing step. The third column shows the equipment used to carry out each fabrication process step. The last column is the cost of each process in US dollars. The values in this column were calculated by multiplying the electricity consumption of each fabrication instrument (W) by the required time of each process (h), divided by the electricity cost per kWh in our laboratory in Mexico, which is 0.085 $/kWh. Therefore, the fourth column demonstrates the cost of each fabrication process in US dollars. The total manufacturing cost is then obtained from the sum of the values in the last columns of Table S2 and Table S3 for the Registration module. The manufacturing cost of Scribing module was obtained using the sum of the values in the las columns of Table S4 and Table S5. The total cost of raw materials and fabrication process obtained from Tables S2 to S5 was used to plot Figure 4.

Table S2. Raw materials and components and their corresponding price/kg and the cost of required quantities for the fabrication of the A4 size R module.

Compartment	Raw materials	Price ($/kg)	Required quantity (kg)	Cost/required quantity ($)
Working electrode	FTO glass (TEC-7 2.2 mm)		1pz (275 x 210 mm^2)	22
Electrode cleaning	Soap (Hellmanex)	48	0.00030	0.014
	Deionized water	0.18	0.020	0.0036
	Ethanol	2.5	0.0079	0.020
	Isopropyl alcohol	3.4	0.0079	0.026
	Total			0.063
Blocking layer	* TiACAC	210	0.0025	0.52
	Isopropyl alcohol	3.4	0.018	0.059
	Total			0.58
TiO_2 layer	TiO_2 CINVESTAV paste	1945	0.000067	0.13
	TiO_2 commercial paste	4469	0.000067	0.30
Separator layer	Alumina CINVESTAV paste	1889	0.00016	0.29
	Alumina commercial	9602	0.00016	1.5
	Zirconia commercial	10,147	0.00022	2.2
Carbon layer	Commercial carbon	202	0.0011	0.22
Perovskite precursor solution (one-step)	MAI	1722	0.00014	0.25
	AVAI	9010	0.0000066	0.059
	GBL	66	0.0010	0.067
	PbI_2	1132	0.00042	0.47
	Total			0.84
Perovskite precursor solution (two-step)	PbI_2	1132	0.00042	0.47
	DMF	95	0.00089	0.085
	MAI	1722	0.0023	4.0
	IPA anhydrous	81	0.20	16
	Total			21
Soldering	Sn wire	15	0.0031	0.047

* Titanium diisopropoxide bis (acetylacetonate)

Table S3. Processes and the corresponding costs for the fabrication of the R module.

Manufacturing step	Process	Equipment	* Process cost ($)
FTO	Patterning	Laser Nb: YVO_4 532 nm	0.002
	Cleaning	Plasma cleaner	0.004
	Total		0.006
Blocking layer deposition	Spray pyrolysis	Compressor	0.032
		Hotplate	0.094
	Total		0.13
TiO_2 layer deposition	Deposition	Screen printing	<0.01
		Compressor	0.011
	Drying	Hotplate	0.0080
	Heat treatment	Furnace	0.74
	Total		0.76

Separator layer deposition	Deposition	Screen printing	<0.01
		Compressor	0.011
	Drying	Hotplate	0.0080
	Heat treatment	Furnace	0.59
	Total		0.60
Carbon layer deposition	Deposition	Screen printing	<0.01
		Compressor	0.011
	Drying	Hotplate	0.0080
	Heat treatment	Furnace	0.59
	Total		0.60
Perovskite preparation	Solution preparation	Hotplate	0.75
		Glovebox and balance	0.0028
		Dry room	0.42
	Total		1.2
Perovskite deposition	Infiltration (one/two-step)	Robotic arm	<0.01
		Compressor	0.0053
		Dry room	1.7
		hotplate	0.19
	Total		1.9
Full device	Humidity treatment	Oven	0.17
Full device	Soldering	Ultrasonic soldering	0.0021

* Electricity cost in Merida, Mexico is 0.085 $/kWh.

Table S4. Raw materials and components and their corresponding price/kg and the cost of required quantities for the fabrication of the S module.

Compartment	Raw materials	Price ($/kg)	Required quantity (kg)	Cost/required quantity ($)
Working electrode	FTO glass (TEC-7 2.2 mm)		1pz (220 × 165 mm2)	14
Electrode cleaning	Soap (Hellmanex)	48	0.00030	0.014
	Deionized water	0.18	0.020	0.0036
	Ethanol	2.5	0.0079	0.020
	Isopropyl alcohol	3.4	0.0079	0.026
	Total			0.063
Blocking layer	* TiACAC	210	0.0020	0.42
	Isopropyl alcohol	3.4	0.013	0.048
	Total			0.47
TiO_2 layer	TiO_2 CINVESTAV paste	1945	0.000095	0.18
	TiO_2 commercial paste	4469	0.000095	0.42
Separator layer	Alumina CINVESTAV paste	1889	0.00015	0.27
	Alumina commercial	1014	0.00015	1.4
	Zirconia commercial	10,147	0.00021	2.14
Carbon layer	Commercial carbon	202	0.00085	0.17
Perovskite precursor solution (one-step)	MAI	1722	0.00014	0.25
	AVAI	9010	0.0000066	0.059
	GBL	66	0.0010	0.067
	PbI_2	1132	0.00042	0.47

	Total			0.84
Perovskite precursor solution (two-step)	PbI_2	1132	0.00042	0.47
	DMF	95	0.00089	0.085
	MAI	1722	0.0023	4.0
	IPA anhydrous	81	0.20	16
	Total			21
Soldering	Sn wire	15	0.0035	0.053

* Titanium diisopropoxide bis (acetylacetonate)

Table S5. Processes and the corresponding costs for the fabrication of the S module.

Manufacturing step	**Process**	**Equipment**	*** Process cost ($)**
FTO	Patterning	Laser Nb: YVO_4 532 nm	0.007
	Cleaning	Plasma cleaner	0.004
	Total		0.011
Blocking layer deposition	Spray pyrolysis	Compressor	0.032
		Hotplate	0.094
	Total		0.13
TiO_2 layer deposition	Deposition	Screen printing	<0.01
		Compressor	0.011
	Drying	Hotplate	0.0080
	Heat treatment	Furnace	0.74
	Total		0.76
Separator layer deposition	Deposition	Screen printing	<0.01
		Compressor	0.011
	Drying	Hotplate	0.0080
	Heat treatment	Furnace	0.59
	Total		0.60
Carbon layer deposition	Deposition	Screen printing	<0.01
		Compressor	0.011
	Drying	Hotplate	0.0080
	Heat treatment	Furnace	0.59
	Total		0.60
Perovskite preparation	Solution preparation	Hotplate	0.75
		Glovebox and balance	0.0028
		Dry room	0.42
	Total		1.2
Perovskite deposition	Infiltration (one/two-step)	Robotic arm	<0.01
		Compressor	0.0053
		Dry room	1.7
		hotplate	0.19
	Total		1.9
Full device	Humidity treatment	Oven	0.17
Full device	Soldering	Ultrasonic soldering	0.0021

* Electricity cost in Merida, Mexico is 0.085 $/kWh.

- **Titania nanoparticle synthesis and paste preparation**

TiO_2 nanoparticles were synthesized using sol-gel method as described previously. In summary, acetic acid (≥99.7%, Sigma-Aldrich) was added to titanium (IV) isopropoxide (TIP) (>97%, Sigma-Aldrich), and the solution was stirred for 2 minutes. Then the mixture was added dropwise to deionized water with constant stirring. Nitric acid (ACS reagent, 70%, Sigma-Aldrich) was added to the mixture, which was subsequently heated to 80 °C and the suspension was peptized for 75 min. The resultant colloid was hydrothermally treated at 200 °C for 24 h in a Teflon-lined autoclave (Parr Instruments). The final product was washed and centrifuged (Thermo Scientific ST8 Benchtop) with ethanol. A screen-printing paste was obtained by preparing two solutions: (1) ethyl cellulose (EC) (100 cP Sigma-Aldrich) in ethyl alcohol (CTR scientific) and (2) TiO_2 as it was obtained, in ethanol. The resulting suspensions were stirred separately for 1 h. α-Terpineol (Sigma-Aldrich) was added to solution 2 and stirred for 3 min and then sonicated using a probe sonicator (Sonics, VCX750) applying 3 s pulse / 3 s pause for total time of 3 min at 40% amplitude. Then solution 1 was added to the mixture followed by stirring/sonication under the same experimental parameters. The excess ethanol was removed with a rotary evaporator (BUCHI Rotavapor R210) resulting in a diluted TiO_2 screen-printing paste suitable for perovskite solar cell application.

- **Alumina synthesis and paste preparation**

Alumina nanoparticles were synthesized the following way, using a method similar to that reported by Amirsalari and Shayesteh. An aqueous solution of aluminium nitrate nonahydrate (Sigma-Aldrich ≥ 98%) was prepared and heated at 60 °C with constant stirring. The aqueous solution of ammonium hydroxide (Fermont) was added to the first solution at a constant rate with stirring to obtain a pH in the range of 8 to 10. Then the mixture was cooled down to room temperature and centrifuged twice with distilled water. The final product was dried at 110 °C. The dry powder was sintered at 800 °C for 8 h to obtain the final alumina powder. The alumina paste was prepared using the same procedure as for titania paste.

Before preparing the screen-printing pastes for electrode fabrication, the synthesized titania and alumina materials were characterized in powder form using a Siemens D5000 X-ray powder diffraction setup (XRD) to confirm the purity of the phases. Also, the materials morphology was observed using JEOL JSM-7600F field emission scanning electron microscope.

- **Characterization of TiO_2 and Al_2O_3 materials**

Figure S2a shows the XRD patterns of the TiO_2 powder illustrating the main anatase peak at 2θ value of 25.28° corresponding to (101) plane. Also, the two other intense peaks at 37° and 48° corresponding to the (004) and (200) planes, respectively, show the tetragonal structure of the synthesized material. The inset of the Figure shows the SEM image of titania powder. The anatase nanoparticles are spherical with a size distribution in the range of 15 to 33 nm (diameter) and an average size of about 22 nm. In Figure S2b, it can be observed that the XRD peak positions of the alumina matches with the γ-alumina phase. The peaks at 37.2°, 45.6° and 66.9° correspond to the (311), (400) and (440) planes, respectively. The inset of the Figure shows the SEM image of alumina powder, illustrating a morphology that can be described as agglomerations of microcubes.

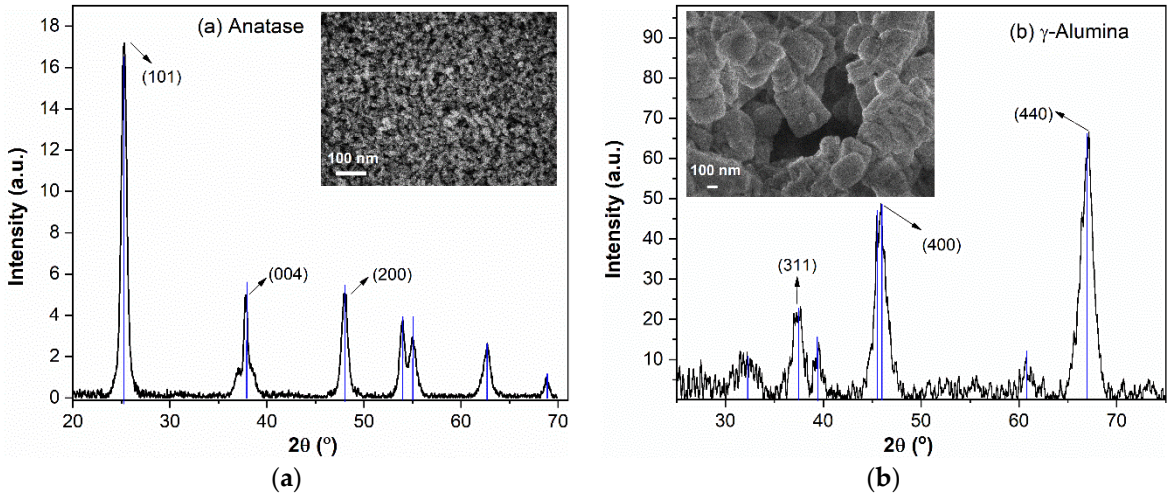

Figure S2. (a) X-ray diffraction pattern of TiO_2 powder synthesized in this work; the inset shows the corresponding SEM image; **(b)** X-ray diffraction pattern of the Al_2O_3 material synthesized with the SEM image of the alumina powder in the inset.

- **Cost analysis: titania and alumina pastes**

The bottom-up cost analysis method was used to estimate the cost of titania and alumina pastes. The pastes are prepared starting from nanoparticle synthesis followed by aggregation of organic binders to obtain the proper rheological characteristics for screen printing. The cost of prepared titania and alumina pastes was calculated for 1 kg of the final product and compared with the same quantity of commercially available pastes. All raw materials were purchased from Sigma-Aldrich except deionized water and ethanol, which were bought from local companies. The tax and shipping were included in raw material purchasing price. The raw materials are sold in different quantity units such as g, L or mL. To ensure the accurate comparison of the purchasing price of different materials, the quantity is presented in kg for all materials, including for liquids by using their density to calculate the weight, and the purchasing price for 1 kg of material was determined. For the marketable production of the pastes, costs such as capital, labour, utilities, equipment maintenance and depreciation were included in our calculations. The pastes final prices were compared with the commercially available pastes.

Note that to investigate the performance of the solar cells using our pastes, the commercial titania and zirconia were replaced with home-made titania and alumina, respectively. The purchasing price of the commercially available zirconia and alumina is very similar, and although in this work the commercial alumina was not used for solar cell manufacturing, its price is shown in Table S6 for comparison.

Table S6. The cost comparison between the pastes prepared in this work and commercially available pastes for 1 kg of the final product, for availability in Mexico.

Product	[2] **Paste manufacturing cost ($)**	[3] **Paste purchasing price ($)** (Website price)	**Shipping cost ($)**	**Importation cost ($)**	[4] **Total Purchasing price ($)** (After shipping & Importation)
CINVESTAV titania paste	1620	* 1945	No applicable	No applicable	No applicable
CINVESTAV alumina paste	1575	* 1890	No applicable	No applicable	No applicable
Commercial titania paste [1]	No data	3040	152	1276.8	4469
Commercial alumina paste [1]	No data	6532	326.6	2743.44	9603
Commercial zirconia paste [1]	No data	6903	345.15	2899.26	10,147

1. The commercial titania and alumina/zirconia pastes were purchased from GreatCell Solar and Solaronix, respectively.

2. Paste manufacturing cost was calculated for home-made pastes considering capital cost, labour cost, utilities, equipment cost, maintenance, and depreciation. For the commercially available pastes these values are unknown.
3. This is the purchasing price provided by the manufacturer companies.
4. This is the total purchasing price after 5% shipping and 40% importation of the products to Mexico.

* For the home made pastes, the purchasing price is suggested by us.

Figure S3a shows the materials cost distribution for the products presented in Table S6. Figure S3b and S3c show the breakdown into the main cost components for the home-made pastes. In Figure S3a, the product cost (blue column) of commercially available pastes is much higher than that of the pastes prepared in-house. This may be partially due to the small batch sizes, and high wage rates, including for transportation of raw materials, utilities, land and local taxes in the country of manufacture.

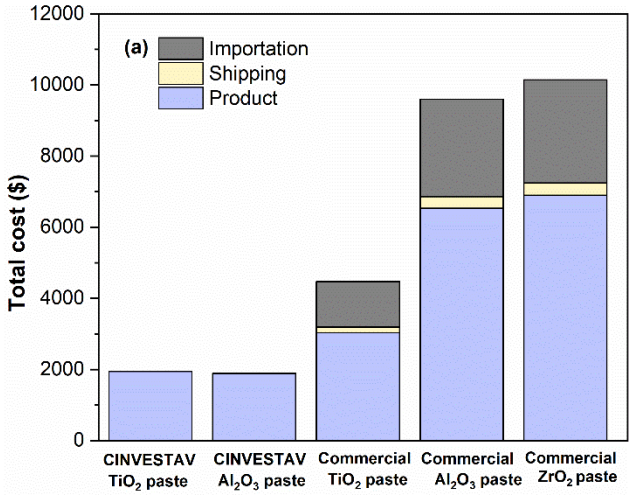

(**a**)

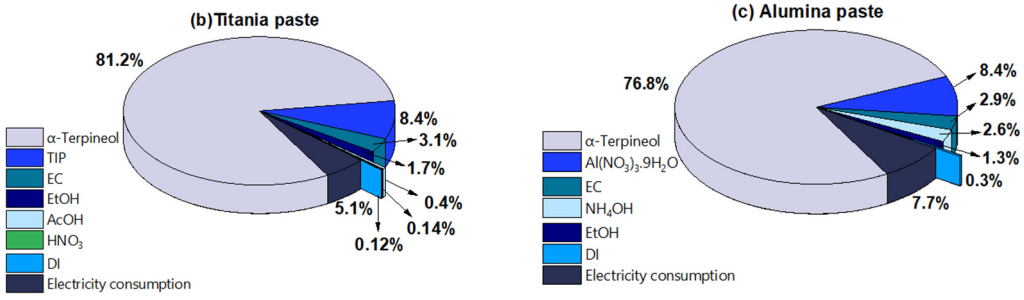

(**b**) (**c**)

Figure S3. (a) Cost comparison of the prepared pastes and the commercially available pastes; **(b)** and **(c)** Cost breakdown for the titania and alumina pastes, respectively.

- **Single solar cell fabrication process**

Fluorine-doped tin oxide (FTO) on glass (XOP Glass) with a sheet resistance of 7 Ω/□ was used as substrate, and was first patterned using a Nb:YVO_4 laser (532 nm). Then the substrate was washed with 2% (v/v) solution of Hellmanex in deionized water, rinsed with acetone and isopropyl alcohol (IPA) and finally plasma-cleaned in O_2 atmosphere for 5 min. The blocking layer was deposited by spray pyrolysis from a 4% (v/v) solution of titanium diisopropoxide bis(acetylacetonate) (75% in IPA, Sigma-Aldrich) in IPA onto the

substrate at 300 °C. After applying a spray coating 30 times the substrate was heated to 500 °C for 30 min to obtain an approximately 50 nm thickness. Four series of devices were fabricated using different pastes as shown in Table S7. The commercial titania paste (30NR-D, GreatCell Solar) was first diluted in α-terpineol in a 1:1 weight ratio before screen printing. The prepared TiO_2 and diluted commercial titania paste was deposited in a square area of 1 cm^2 using a semi-automatic screen printer (ATMA: AT-25PA Digital Electric Flat Screen Printer) and the layers were sintered at 550 °C for 30 min. Then the zirconia (Zr-Nanoxide ZT/SP, Solaronix) and prepared alumina pastes were deposited on top of the titania layers followed by heat treatment at 400 °C for 30 min. As the last layer, carbon paste (Gwent electronic materials) was screen printed on top of the previous layer and thermally treated at 400 °C for 30 min. The final films thickness was measured using Veeco Dektak 150 with a probe of radius 12.5 μm and is shown in Table S7. A solution of lead iodide (99% Sigma-Aldrich), methyl ammonium iodide (CH_3NH_3I, GreatCell Solar), 5-ammonium valeric acid iodide (5-AVAI) ($C_5H_{12}INO_2$, GreatCell Solar) was prepared in γ-butyrolactone (GBL) ($C_4H_6O_2$, Sigma-Aldrich). The solution composition was 439 mg PbI_2, 151.4 mg MAI and 6.7 mg 5-AVAI in 1 mL GBL and it was left at 50 °C under stirring and inside the glovebox overnight. A one-step perovskite deposition method was applied under a low humidity ambient (30% RH) in which an 8 μL drop of the solution was cast on the surface of the carbon layer at room temperature. After allowing the solution to infiltrate through the triple stack for 10 min, the electrodes were annealed in a fan oven at 50 °C for 2 h. Then the devices were treated at 70% relative humidity (RH) and 25 °C for 24 h. The excess perovskite was removed from the contact areas and a low-temperature solder wire was soldered using MBR electronics ultrasonic soldering device. The devices were measured in dark and after 3 min of 1 sun light soaking using a Sol3A from MKS Newport with AM1.5G filter. The cell area of 0.49 cm^2 was exposed to the light by masking each device.

- **Solar cell performance**

To investigate the performance of our pastes, 4 series of devices were fabricated as explained. Figure S4 shows the performance of the solar cells after 24 hours humidity treatment and 3 min of light soaking before the measurements. In each experimental series, 3 identical solar cells were fabricated. Devices with the commercial titania, zirconia and carbon were considered as the standard devices (Std Device). In category A devices, the home-made titania paste was used, and the two other layers were printed from the commercially available pastes. For B series devices, the alumina layer was printed from the home-made paste, and titania and carbon layers from the purchased pastes. Finally, the C devices were fabricated using home-made titania and alumina pastes, and the Gwent commercial carbon paste (see Table S7). The squares in Figure S4 indicate the average values for each parameter listed in Table S8.

For cells performance, the JV curves were obtained, and the photovoltaic parameters were calculated using the following formula 1:

$$PCE(\eta) = FF\frac{J_{SC} \times V_{OC}}{P_{in}} \quad (1)$$

where PCE is power conversion efficiency, FF is the fill factor, J_{SC} and V_{OC} are the short-circuit current density and open-circuit voltage, respectively. The P_{in} is the input power, and it equals 1 sun or 1000 W/m^2.

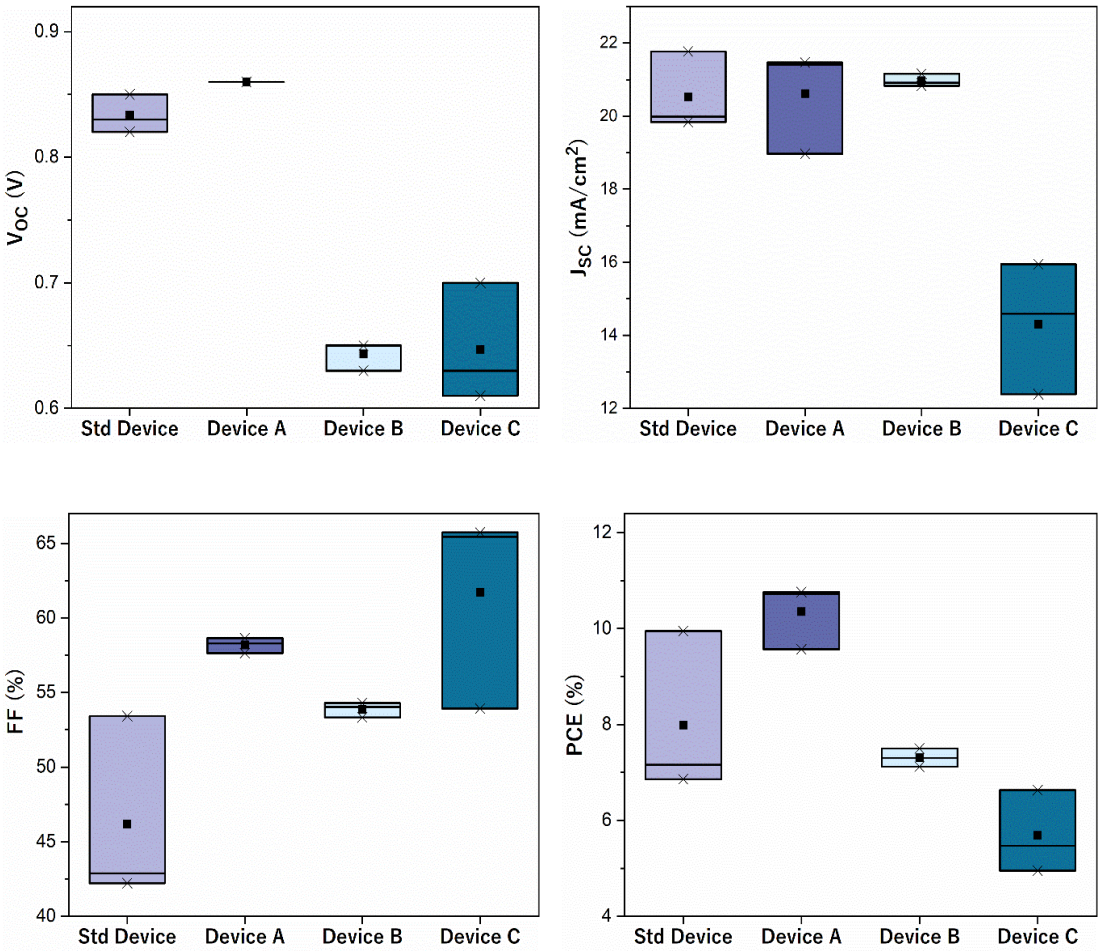

Figure S4. Box chart of photovoltaic parameters of three series of devices compared to the standard device: Std device: triple stack of commercial pastes; Device A: home-made titania and commercial zirconia and carbon, Device B, home-made alumina and commercial titania and carbon; Device C: home-made titania and alumina and commercial carbon.

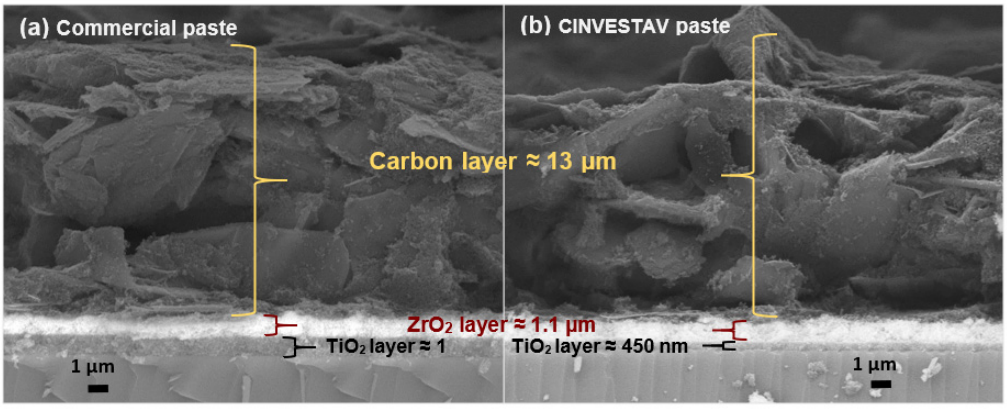

Figure S5. Titania layer deposited on the glass/FTO substrate from: **(a)** GreatCell Solar titania paste; **(b)** CINVESTAV paste.

Table S7. Triple stack composition and the final films thickness for four series of fabricated devices as standard (Std), A, B and C-series devices.

Device	TiO_2 layer		Separator layer		Carbon layer	
	Source	Thickness (μm)	Source	Thickness (μm)	Source	Thickness (μm)
Std	Commercial	≈1	Commercial	≈1.1	Commercial	≈13
A	In-house	≈0.45	Commercial	≈1.1	Commercial	≈13
B	Commercial	≈1	In-house	≈3	Commercial	≈13
C	In-house	≈0.45	In-house	≈3	Commercial	≈13

Table S8. Photovoltaic parameters for fabricated cells with different pastes. The average values for three measured cells for each series devices and the corresponding standard deviation are given.

Device	VOC (V)	JSC (mA/cm²)	FF (%)	PCE (%)
Std	0.83 ± 0.012	21 ± 0.88	46 ± 5.1	8.0 ± 1.4
A	0.86 ± 0	21 ± 1.2	58 ± 0.42	10.4 ± 0.55
B	0.64 ± 0.0094	21 ± 0.14	54 ± 0.41	7.3 ± 0.16
C	0.65 ± 0.039	14 ± 1.5	62 ± 5.5	5.7 ± 0.70

The A series devices have shown the best performance in terms of efficiency, which we relate to the observation that the titania layer from the home-made paste is about half the thickness compared to the film from the commercial paste. The thickness of the titania layer is an important factor for the electron transport properties, also related to the success of infiltration of the perovskite; hence, thinner layers may be advantageous. The thickness of the titania layer depends on the rheological parameters, including the viscosity. The rheological parameters of the home-made paste were optimized in order to be able to print thin films. Although the commercial paste was diluted in 1:1 weight ratio with terpineol, the film thickness still was about twice as large (see Figure S5) using the same screen printing parameters, such as screen mesh size, squeegee type, speed and angle, and the gap between the screen and the substrate. The commercially available titania paste is very viscous as-received, and the extra step must be carried out in order to prepare a diluted paste and obtain a thinner layer. The dilution component is terpineol, which accounts for more than 80% of the paste cost contribution (see Figure S3b). Hence, beside the high cost of commercially available paste itself, the cost of the extra step must be considered. It is worth mentioning that the 1:1 (α-terpineol: viscous paste) weight ratio is the optimum ratio proposed by different research groups for screen printing and is used in this work. It is possible to further dilute the commercial paste, however two issues must be addressed: (1) the cost of this extra step and (2) the rheological properties of a very diluted paste. The cost of extra step includes the cost of viscous paste and additional α-terpineol, as well as the electricity consumption for the mixing process. The increase in terpineol and decrease in viscous paste quantities may balance the total cost of diluted paste, however, it is still significantly more expensive than the cost of home-made paste. Besides, any extra step in fabrication process is time-consuming and slows the production rate. On the other hand, the rheological properties of a very diluted paste must be investigated and optimized. Since for carbon-based perovskite solar cell fabrication, the screen printing technique is used, all three pastes must be easily printable. A very viscous paste results in a thick film and a very diluted paste may cause printing issues such as penetration of the ink through the screen and inhomogeneous deposition. These issues could potentially be solved by modifying the screen printing parameters, which was beyond the scope of this work. Our results illustrate the advantages of developing a home-made paste specifically for application in printed perovskite solar cells, not just from a cost point of view, but also to optimize performance without using any extra fabrication step.

By using the alumina paste in B and C devices, the open circuit voltage decreases approximately 200 mV compared with the Std and A devices, where commercial zirconia is used. We believe that this is related with the thickness of the alumina layer as compared to that of the zirconia layer: in the B and C devices, the thickness of the alumina layer was 3 μm while the zirconia layer in Std and A devices was 1.1 μm; the optimum value reported in literature is around 2 μm. The large separator film thickness allows for enhanced recombination thus lowering the V_{OC}. However, in general it can be concluded that the performance of the alumina-based solar cells was only slightly less than that of the standard cells, which indicates the promise of the home-made alumina paste. To improve the performance of the alumina-based devices, further modification of the paste rheology and screen printing parameters must be carried out in order to obtain the optimum alumina layer thickness. Up to our knowledge, the performance of the alumina-based perovskite solar cells using 5-AVAI has not reported yet. Investigations in this area must be addressed to understand the 2D/3D perovskite infiltration and growth mechanism through the alumina layer.